ORMDL proteins regulate ceramide levels during sterile inflammation

Lin Cai,[1,*,†] Clement Oyeniran,[1,†] Debolina D. Biswas,[†] Jeremy Allegood,[†] Sheldon Milstien,[†] Tomasz Kordula,[†] Michael Maceyka,[†] and Sarah Spiegel[2,†]

School of Pharmacy,* Wenzhou Medical University, Wenzhou, Zhejiang 325035, China; and Department of Biochemistry and Molecular Biology and the Massey Cancer Center,[†] Virginia Commonwealth University School of Medicine, Richmond, VA 23298

Abstract The bioactive sphingolipid metabolite, ceramide, regulates physiological processes important for inflammation and elevated levels of ceramide have been implicated in IL-1-mediated events. Although much has been learned about ceramide generation by activation of sphingomyelinases in response to IL-1, the contribution of the de novo pathway is not completely understood. Because yeast ORM1 and ORM2 proteins negatively regulate ceramide levels through inhibition of serine palmitoyltransferase, the first committed step in ceramide biosynthesis, we examined the functions of individual mammalian ORM orthologs, ORM (yeast)-like (ORMDL)1–3, in regulation of ceramide levels. In HepG2 liver cells, downregulation of ORMDL3 markedly increased the ceramide precursors, dihydrosphingosine and dihydroceramide, primarily from de novo biosynthesis based on [U-^{13}C]palmitate incorporation into base-labeled and dual-labeled dihydroceramides, whereas downregulation of each isoform increased dihydroceramides [^{13}C]labeled in only the amide-linked fatty acid. IL-1 and the IL-6 family cytokine, oncostatin M, increased dihydroceramide and ceramide levels in HepG2 cells and concomitantly decreased ORMDL proteins. Moreover, during irritant-induced sterile inflammation in mice leading to induction of the acute-phase response, which is dependent on IL-1, expression of ORMDL proteins in the liver was strongly downregulated and accompanied by increased ceramide levels in the liver and accumulation in the blood. Together, our results suggest that ORMDLs may be involved in regulation of ceramides during IL-1-mediated sterile inflammation.—Cai, L., C. Oyeniran, D. D. Biswas, J. Allegood, S. Milstien, T. Kordula, M. Maceyka, and S. Spiegel. **ORMDL proteins regulate ceramide levels during sterile inflammation.** ***J. Lipid Res.*** **2016.** 57: **1412–1422.**

Supplementary key words serine palmitoyltransferase • ORM-like protein • ceramide synthase • sphingolipids

This work supported by National Institutes of Health Grants R37GM043880 and R01 AI50094 (S.S.), and 1R01AI093718 (T.K.). L.C. was supported by National Natural Science Foundation of China (81101570). The content is solely the responsibility of the authors and does not necessarily represent the official views of the National Institutes of Health. The VCU Lipidomics Core was supported in part by the Massey Cancer Center with funding from the National Cancer Institute grant P30 CA016059.The authors declare that they have no competing financial interests.

Manuscript received 17 December 2015 and in revised form 21 May 2016.

Published, JLR Papers in Press, June 16, 2016
DOI 10.1194/jlr.M065920

Originally sphingolipids were considered to be building blocks of all eukaryotic cell membranes. However, recent advances in our knowledge of sphingolipid metabolism, development of state of the art sphingolipidomic techniques, and knockout of key sphingolipid metabolic enzymes in mice have convincingly illustrated that ceramide, a metabolite of all sphingolipids, is a bioactive lipid that regulates a diverse range of cellular processes, including those important for inflammation [reviewed in (1, 2)]. Indeed, several pro-inflammatory cytokines, including IL-1, increase ceramide levels in diverse cell types (1). IL-1 plays an important role in both inflammatory and immune responses to infections or sterile insults and subsequent induction of acute-phase response (APR) (3, 4). APR is an early innate physiological reaction occurring soon after the onset of infection, trauma, and inflammatory processes resulting in fever, increased vascular permeability, muscle and joint pain, and a variety of metabolic and pathologic changes. The liver is the major organ targeted by IL-1 and members of the IL-6 cytokine family during APR resulting in dramatic increases in synthesis of acute phase proteins (APPs) such as α-1-acid glycoprotein, C-reactive protein, and serum amyloid-A (SAA) in humans and mice (5).

It has been suggested that ceramide generated from degradation of sphingomyelin by activation of neutral or acidic sphingomyelinases mediates some of the pleiotropic responses to IL-1 (6–9). There is also some evidence implicating enhanced de novo ceramide biosynthesis and effects on serine palmitoyltransferase (SPT) leading to increased ceramide levels by IL-1 and during APR (10, 11).

SPT is a key enzyme and the first committed step in the biosynthesis of ceramide and complex sphingolipids derived from ceramide, and several new subunits and

Abbreviations: APP, acute phase protein; APR, acute-phase response; dihydro-S1P, dihydrosphingosine-1-phosphate; ORMDL, ORM (yeast)-like protein; OSM, oncostatin M; QPCR, quantitative PCR; SAA, serum amyloid A; SPT, serine palmitoyltransferase; S1P, sphingosine-1-phosphate; VCU, Virginia Commonwealth University.

[1] L. Cai and C. Oyeniran contributed equally to this work.
[2] To whom correspondence should be addressed.
e-mail: sarah.spiegel@vcuhealth.org

regulatory proteins that regulate its activity have recently been described [reviewed in (12)]. Extensive studies in yeast have elegantly demonstrated that the ORM1 and ORM2 proteins interact with and negatively regulate SPT (13–18). Moreover, it was shown that TORC1 and TORC2 protein kinase complexes are involved in phosphorylation of ORM proteins to adjust sphingolipid synthesis and coordinate cell growth with environmental cues, such as nutrient accessibility and stress (17, 18). In mammalian cells, the three homologs, ORM (yeast)-like (ORMDL)1–3, have also been implicated in regulation of SPT activity and ceramide biosynthesis (13, 19–21). However, in contrast to their yeast orthologs, similar phosphorylations of ORMDL proteins cannot be involved in regulating SPT, as they lack the N-terminal phosphorylated region described in yeast ORMs. Moreover, although silencing of expression of all three ORMDLs in cell culture was shown to increase ceramide (13, 20–22), not much is known of the functions of the individual endogenous ORMDL proteins in regulation of ceramide levels. Here we determined the functions of ORMDL1–3 in human HepG2 cells, examined changes in their expression levels in response to key pro-inflammatory cytokines important for APR, and studied changes in ORMDL expression and ceramide levels in IL-1-mediated sterile inflammation in mice.

MATERIALS AND METHODS

Turpentine-induced inflammation

C57BL/6 mice were obtained from Jackson Laboratory (Bar Harbor, ME). All animal studies were conducted in the Animal Research Core Facility at Virginia Commonwealth University (VCU) School of Medicine in accordance with the institutional guidelines. Animals were bred and maintained in a pathogen-free environment and all procedures were approved by the VCU Institutional Animal Care and Use Committee, which is accredited by the Association for Assessment and Accreditation of Laboratory Animal Care. All mice were kept on a 12 h light-dark cycle with free access to food and water. Turpentine abscesses were initiated by sc injection of pure gum spirits of turpentine (50 μl) into anesthetized male and female mice (6–8 weeks of age) (23). Mice were euthanized after 8 or 24 h, and livers were collected for mRNA, lipid, and protein analyses.

Cell culture and transfection

Human hepatoma HepG2 cells (ATCC, Manassas, VA) were cultured in DMEM supplemented with 10% FBS, penicillin, streptomycin, and L-glutamine. Cells were transferred to 12-well dishes and starved in DMEM containing 0.5% FBS for at least 12 h before stimulation. Cells were stimulated with 25 ng/ml IL-1 and 25 ng/ml oncostatin M (OSM) (R&D Systems, Minneapolis, MN) where indicated.

HepG2 cells were transfected with ON-TARGETplus SMARTpool siRNA oligonucleotides (Dharmacon, Lafayette, CO) for human ORMDL1 (catalog number L-018403-01), ORMDL2 (catalog number L-017035-02), and ORMDL3 (catalog number L-01002-02) or scrambled siRNA (siControl) using Lipofectamine RNAiMAX transfection reagent (Life Technologies, Carlsbad, CA).

Quantitative real-time PCR

Total RNA was prepared utilizing TRIzol (Life Technologies). One microgram of RNA was reverse transcribed using the high-capacity cDNA Archive kit (Life Technologies). Premixed primer-probe sets and TaqMan Universal PCR Master Mix (Life Technologies) were employed to examine mRNA levels. cDNAs were diluted 10-fold (for target genes) or 100-fold (for GAPDH) and amplified using the CFX Connect real-time PCR detection system (Bio-Rad). Gene expression levels were calculated by the ΔΔCt method, normalized to *Gapdh* expression, and presented as fold of mean values ± SEM.

Western blotting

Cells were lysed in 10 mM Tris (pH 7.4), 150 mM sodium chloride, 1 mM EDTA, 0.5% Nonidet P-40, 1% Triton X-100, 1 mM sodium orthovanadate, 0.2 mM PMSF, and 1:500 protease inhibitor mixture (Sigma, St. Louis, MO). Equal amounts of protein were separated by SDS-PAGE, transblotted to nitrocellulose, and incubated with primary antibodies against ORMDL3 (1:3,000; Abgent, San Diego, CA) and tubulin (1:8,000; Cell Signaling, Danvers, MA). Immunopositive bands were visualized by enhanced chemiluminescence using secondary antibodies conjugated with horseradish peroxidase (goat anti-rabbit, 1:5,000; Jackson ImmunoResearch, West Grove, PA) and Super-Signal West Pico chemiluminescent substrate (Pierce, Rockford, IL) as described (20). Optical densities of bands associated with proteins of interest were quantified using Image J software and normalized to the optical densities of their respective tubulin bands.

Quantification of sphingolipids by mass spectrometry

Internal standards for mass spectrometry were purchased from Avanti Polar Lipids (Alabaster, AL) and added to samples in 20 μl ethanol:methanol:water (7:2:1) as a cocktail of 500 pmol each. Standards for sphingoid bases and sphingoid base 1-phosphates were 17-carbon chain length analogs: C17-sphingosine; C17-dihydrosphingosine; C17-sphingosine-1-phosphate (S1P); and C17-dihydrosphingosine-1-phosphate (dihydro-S1P). Standards for N-acyl sphingolipids were C12-fatty acid analogs: C12-Cer, N-(dodecanoyl)-sphing-4-enine (d18:1/C12:0); C12-Cer 1-phosphate, N-(dodecanoyl)-sphing-4-enine-1-phosphate (d18:1/C12:0-Cer1P); C12-sphingomyelin, N-(dodecanoyl)-sphing-4-enine-1-phosphocholine (d18:1/C12:0-SM); and C12-glucosylceramide, N-(dodecanoyl)-1-β-glucosyl-sphing-4-enine.

Lipids were extracted from cells and liver tissues. Samples were collected into 13 × 100 mm borosilicate tubes with a Teflon-lined cap (VWR, West Chester, PA). Then 2 ml of CH_3OH and 1 ml of $CHCl_3$ were added together with the internal standard cocktail. The contents were dispersed by sonication at room temperature for 30 s. The single phase mixtures were incubated at 48°C overnight. After cooling, 150 μl of 1 M KOH in CH_3OH was added and, after brief sonication, incubated in a shaking water bath for 2 h at 37°C to cleave potentially interfering glycerophospholipids. The extracts were brought to neutral pH with 12 μl of glacial acetic acid, centrifuged in a table-top centrifuge, and the supernatants transferred to new tubes. The extracts were reduced to dryness using a speed vac. The dried residues were reconstituted in 0.5 ml of the starting mobile phase solvent for LC-ESI-MS/MS analysis, sonicated for 15 s, and then centrifuged for 5 min before transfer of the clear supernatants to autoinjector vials for analysis.

Sphingolipids were separated by reverse-phase HPLC using a Shimadzu Nexera LC-30 AD binary pump system coupled to a SIL-30AC autoinjector and $DGU20A_{5R}$ degasser. The column used was a Supelco 2.1 (i.d.) × 50 mm Ascentis Express C18 column (Sigma) with a binary solvent system at a flow rate of 0.5 ml/min with a column oven set at 35°C. Prior to injection of samples,

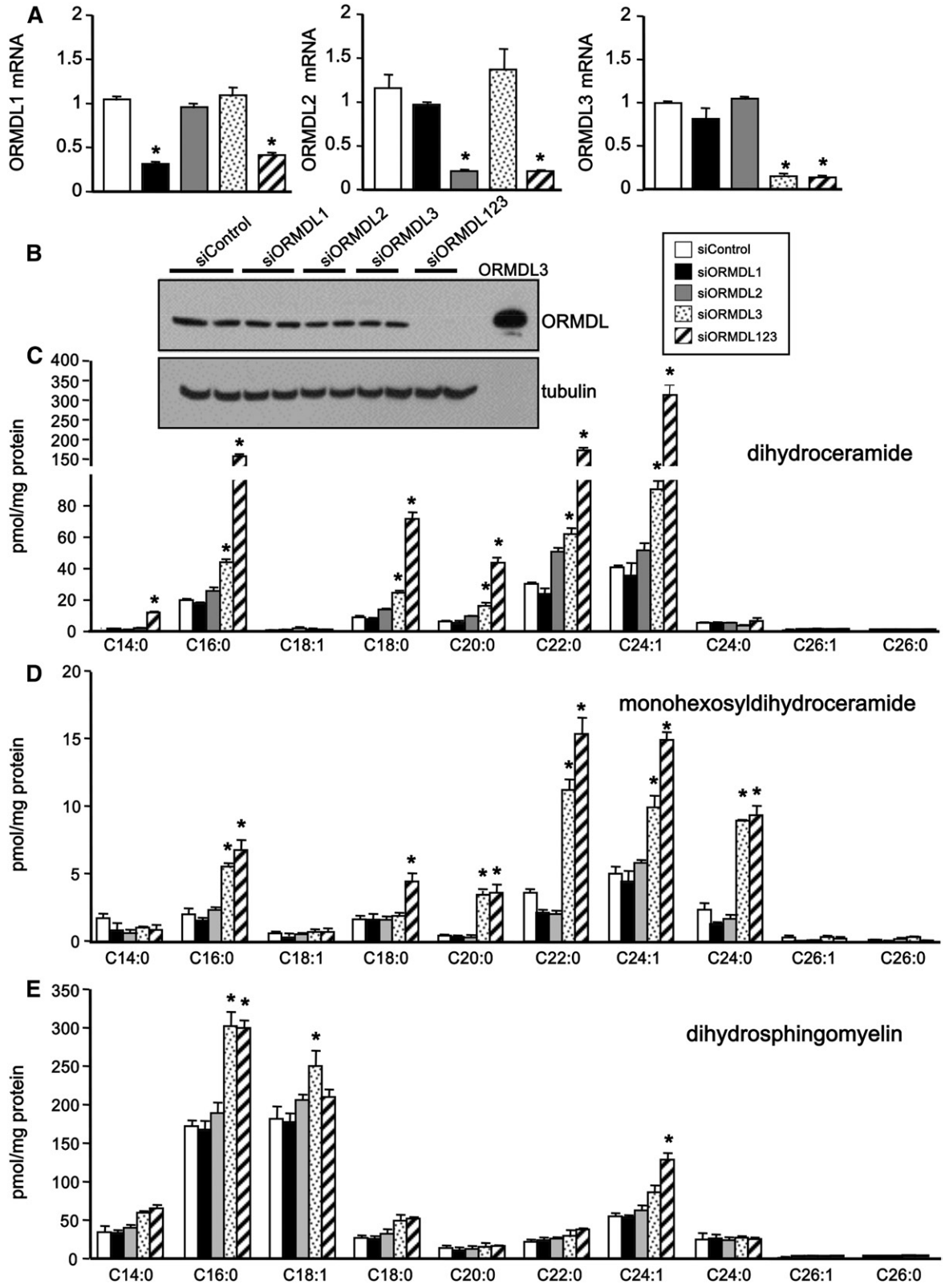

Fig. 1. Downregulation of individual ORMDLs decreases their mRNA levels, but only siORMDL3 increases dihydroceramides. HepG2 cells were transfected with siControl, specific siRNAs for each ORMDL isoform, or with siRNA for all three isoforms as indicated. A: mRNA levels of individual ORMDL isoforms were determined by QPCR and normalized to Gapdh. B: Cell lysates were analyzed by immunoblotting with ORMDL3 antibody. Blots were probed with anti-tubulin antibody to ensure equal loading and transfer. C–E: Lipids were extracted and levels of dihydroceramide (C), monohexosyldihydroceramide (D), and dihydrosphingomyelin (E) species were measured by LC-ESI-MS/MS. Data are mean ± SD (n = 3). $*P < 0.01$ compared with siControl. Similar results were observed in three independent experiments.

the column was equilibrated for 0.5 min with a solvent mixture of 95% mobile phase A1 ($CH_3OH/H_2O/HCOOH$, 58/41/1, v/v/v, with 5 mM ammonium formate) and 5% mobile phase B1 ($CH_3OH/HCOOH$, 99/1, v/v, with 5 mM ammonium formate), and after sample injection (typically 40 μl), the A1/B1 ratio was maintained at 95/5 for 2.25 min, followed by a linear gradient to 100% B1 over 1.5 min, which was held at 100% B1 for 5.5 min, followed by a 0.5 min gradient return to 95/5 A1/B1. The column was re-equilibrated with 95:5 A1/B1 for 0.5 min before each run. The HPLC column was coupled to an AB Sciex 5500 quadrupole/linear ion trap (QTrap; SCIEX Framingham, MA) operating in triple quadrupole mode. Q1 and Q3 were set to pass molecularly distinctive precursor and product ions (or a scan across multiple *m/z* in Q1 or Q3), using N_2 to collisionally induce dissociations in Q2 (which was offset from Q1 by 30–120 eV). The ion source temperature was set at 500°C.

For analysis of de novo sphingolipid synthesis, HepG2 cells were transfected with siRNA as above for 48 h, washed and then incubated for 6 h in medium containing 0.1 mM uniformly labeled [U-^{13}C]palmitate (Sigma) in a 1:1 molar complex with fatty acid-free BSA, as previously described (24, 25). Lipids were extracted and [^{13}C]labeled sphingolipids quantified by LC-ESI-MS/MS.

Statistical analyses

Statistical analysis was performed using two-way ANOVA followed by post hoc tests for experiments consisting of three or more groups (Prism; GraphPad Software, La Jolla, CA). $P < 0.01$ was considered to be statistically significant. All experiments were repeated at least three times with consistent results. For mouse studies, three to six randomly chosen mice were used per experimental group.

RESULTS

Downregulation of ORMDL3, but not ORMDL1 or -2, increases dihydroceramide

Yeast ORM1 and -2 proteins have been reported to bind to and inhibit SPT, the rate-limiting step in de novo ceramide synthesis (13–18), and their human orthologs, ORMDL1, -2, and -3, are thought to have a similar function in mammalian cells. However, the functions of individual ORMDL isoforms in regulation of sphingolipid biosynthesis and ceramide levels are still not clear. For example, whereas one study suggested that each of the ORMDL isoforms can inhibit SPT activity in cells (26), in another study, coordinated overexpression of all three isoforms, but not individual ORMDLs, inhibited de novo ceramide synthesis (21). Therefore, we examined the effects of downregulating individual ORMDLs in HepG2 liver cells,

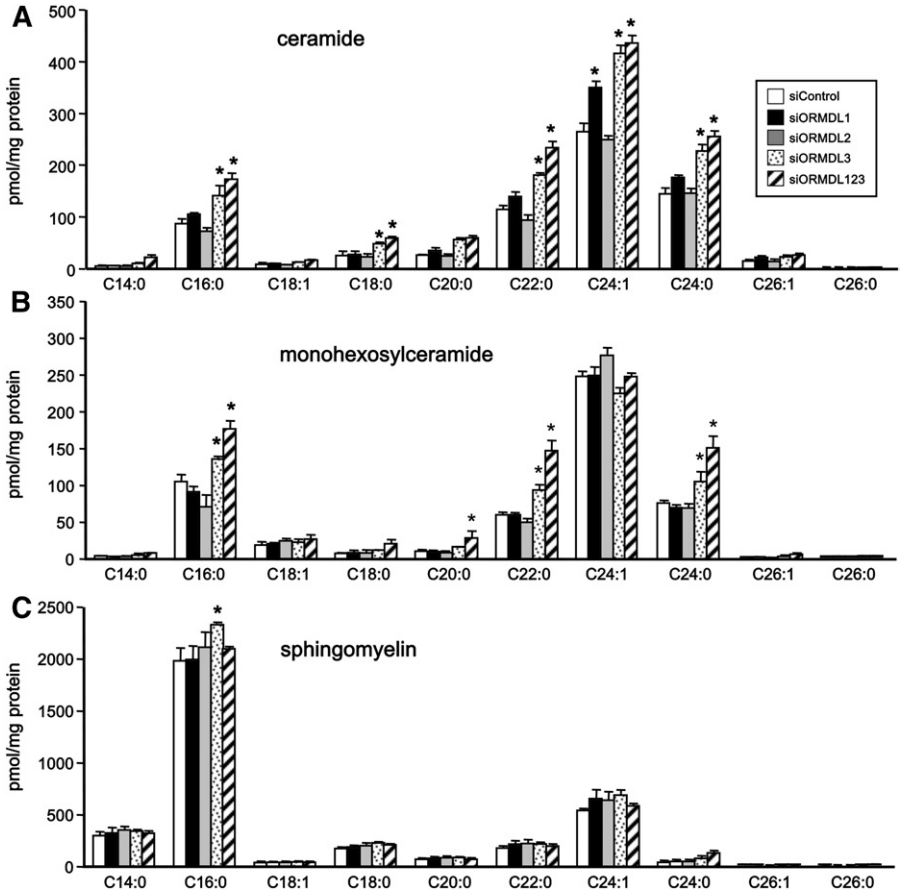

Fig. 2. Downregulation of ORMDL1 and ORMDL3 increases ceramide and complex sphingolipids. HepG2 cells were transfected with siControl, specific siRNAs for each ORMDL isoform, or with siRNA for all three isoforms as indicated. A–C: Lipids were extracted and ceramide (A), monohexosylceramide (B), and sphingomyelin (C) species were quantified by LC-ESI-MS/MS. Data are mean ± SD and are representative of three independent experiments. *$P < 0.01$ compared with siControl.

which express all three isoforms, and examined changes in ceramide and sphingolipid levels by a sensitive mass spectrometry method. After transfection with specific siRNAs, expression of each of the individual ORMDLs was efficiently downregulated by more than 60% without significantly affecting the expression of the other two (**Fig. 1A**). Moreover, simultaneous knockdown of all three ORMDLs showed similar reductions in mRNA levels as the individual siRNAs alone. Western blot analysis of cells overexpressing ORMDL3 confirmed that a commercially available anti-ORMDL3 antibody recognized a 17 kDa band corresponding to the molecular weight of ORMDLs (Fig. 1B). Although simultaneous downregulation of all three ORMDLs reduced the ORMDL protein expression below detectable levels, a significant decrease was not observed with individual knockdowns (Fig. 1B). This is probably due to the greater than 80% homology between ORMDL1, -2, and -3.

We first examined the effects of knockdown of ORMDLs on levels of dihydroceramides, intermediates in the de novo pathway. Downregulation of ORMDL3, but not ORMDL1 or ORMDL2, dramatically increased levels of dihydroceramides (Fig. 1C). This increase was especially robust in C16:0, C18:0, C20:0, C22:0, and C24:1 dihydroceramide species (Fig. 1C). There were also large increases in the same species of monohexosyldihydroceramide (Fig. 1D) as well as in C16:0, dihydrosphingomyelin (Fig. 1E). The effects on dihydrosphingomyelins were likely less dramatic due to the large pool of dihydrosphingomyelins within the cell. Additionally, simultaneous knockdown of all three ORMDL proteins had a stronger effect on increasing dihydroceramides and monohexosyldihydroceramides (Fig. 1C, D), albeit to a lesser extent, whereas dihydrosphingomyelins were not further increased by simultaneous downregulation of all three ORMDLs (Fig. 1E).

Effects of downregulation of ORMDLs on ceramide levels

In the de novo sphingolipid biosynthesis pathway, dihydroceramides are direct precursors of ceramides. In agreement with its effect on dihydroceramides, siORMDL3 also significantly increased levels of most ceramide acyl chain species (**Fig. 2A**). Although siORMDL1 did not increase dihydroceramides (Fig. 1C), it did cause a small increase in the level of the very long chain C24:1 ceramide species (Fig. 2A). However, this was not accompanied by significant increases in the levels of further metabolites of ceramide, monohexosylceramide, and sphingomyelin (Fig. 2B, C). In contrast, siORMDL3 caused small elevations of C16:0, C22:0, and C24:0 species of monohexosylceramide and had almost no effects on sphingomyelins (Fig. 2B, C). Moreover, consistent with its lack of effect on dihydroceramides, siORMDL2 did not have a reproducible effect on ceramides (Fig. 2A), monohexosylceramides (Fig. 2B), or sphingomyelins (Fig. 2C). In contrast to the robust effects on dihydroceramides, downregulation of all three ORMDLs had only minor effects on complex sphingolipid levels compared with downregulation of only ORMDL3 alone.

Effects of downregulation of ORMDLs on sphingoid bases

Downregulation of all three ORMDL isoforms increased levels of cellular dihydrosphingosine (**Fig. 3A**), the precursor of dihydroceramides, and also of its phosphorylated form, dihydro-sphingosine-1-phosphate (dihydro-S1P) (Fig. 3B), as well as sphingosine (Fig. 3C) and S1P (Fig. 3D). siORMDL3 alone also increased levels of dihydro-S1P, sphingosine, and S1P (Fig. 3). However, unexpectedly, siORMDL1 also increased levels of sphingosine, even though it had no effect on levels of dihydrosphingosine-containing lipids (Fig. 3). It should be noted that sphingosine is not an

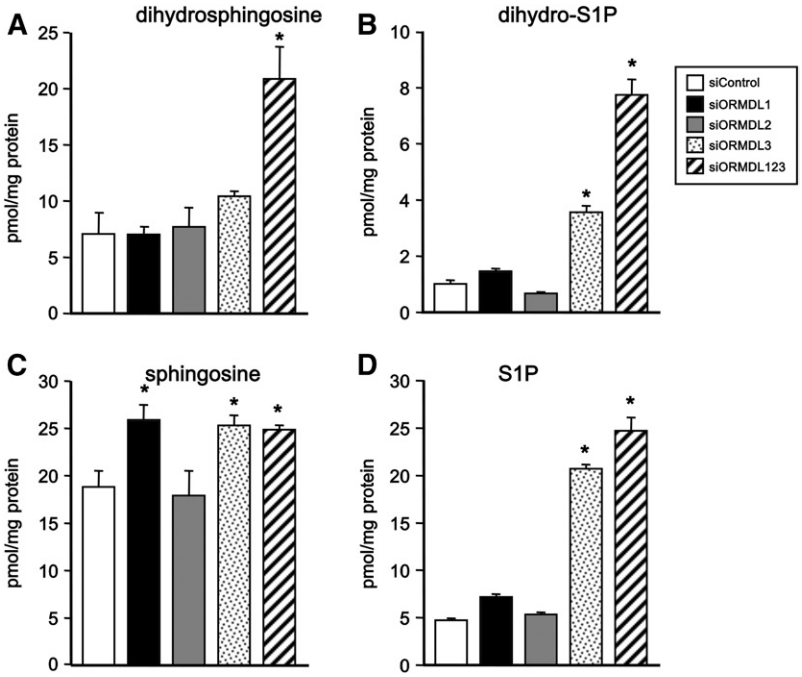

Fig. 3. Effects of downregulation of individual ORMDL isoforms on sphingoid base levels. HepG2 cells were transfected with siControl, specific siRNAs for each ORMDL isoform, or with siRNA for all three isoforms as indicated. A–D: Lipids were extracted and dihydrosphingosine (A), dihydro-S1P (B), sphingosine (C), and S1P (D), were quantified by LC-ESI-MS/MS. Data are mean ± SD. $*P < 0.01$ compared with siControl.

intermediate in the biosynthesis of sphingolipids, but rather a degradation product of ceramide.

Downregulation of ORMDL3 increases de novo sphingolipid synthesis

Given our observed increases in dihydrosphingolipids (Fig. 1) and the reported role of ORMDL proteins in regulating de novo sphingolipid synthesis, we directly followed dihydroceramide biosynthesis by pulse labeling cells with [U-^{13}C]palmitate. This fatty acid is converted into [^{13}C] palmitoyl-CoA, a substrate for SPT, and is also used for N-acylation of dihydrosphingosine to dihydroceramide by ceramide synthases yielding four different isotopically labeled dihydroceramide species: [^{13}C]labeled in the sphingoid base ("base labeled") or with both [^{13}C]labeled sphingoid base and N-acyl chain ("dual labeled"), both indicative of de novo synthesis; [^{13}C] label only in the N-acyl chain ("fatty acid-labeled") and dihydroceramide with only ^{12}C ("unlabeled"), the latter two contain [^{12}C]sphingoid bases that have been released in the recycling/salvage pathway by turnover and then are reacylated with [^{13}C] palmitoyl-CoA or with endogenous unlabeled fatty acyl CoAs, respectively. Consistent with the results shown in Fig. 1, we found that siORMDL3 induced a dramatic increase in [^{13}C] base-labeled and dual-labeled dihydroceramides (**Fig. 4 A, B**). The dihydroceramide species containing only [^{13}C] label in the sphingoid base were proportionately distributed among all N-acyl chain species, as expected, while the predominant dual-labeled species was C16:0 (palmitate) dihydroceramide. Intriguingly, knockdown of either

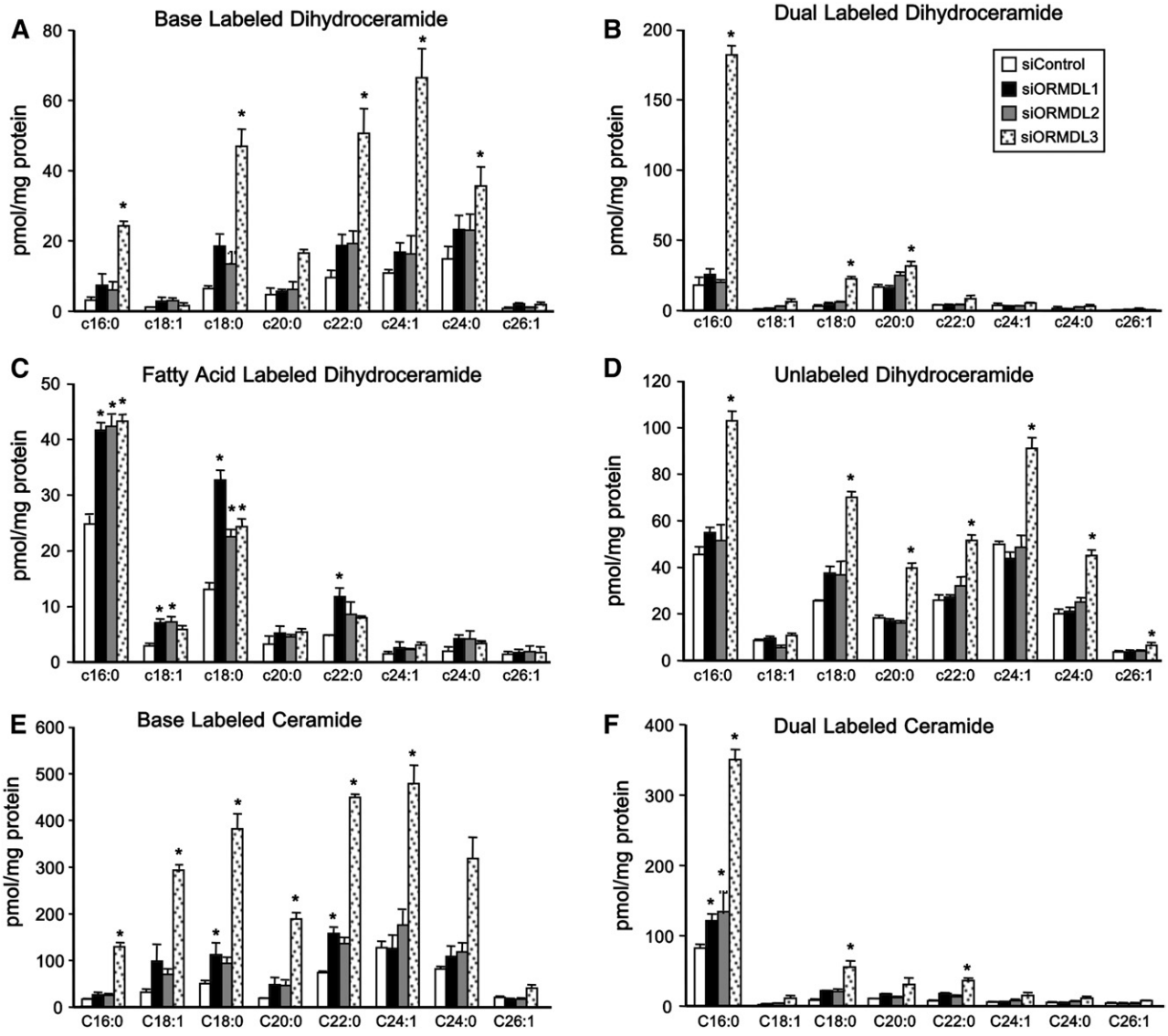

Fig. 4. Downregulation of ORMDL3 increases de novo incorporation of [^{13}C]palmitate into dihydroceramides. HepG2 cells were transfected with the indicated siRNAs for 48 h. Cells were then washed and incubated with uniformly labeled [U-^{13}C]palmitate for 6 h. Sphingolipids were extracted and incorporation of [^{13}C]palmitate into dihydroceramides (A–D) and ceramides (E, F) was determined by LC-ESI-MS/MS. Base-labeled dihydroceramides (A), base and N-acyl chain dual labeled dihydroceramides (B), fatty acid labeled dihydroceramides (C), unlabeled dihydroceramides (D), base-labeled ceramides (E), and dual-labeled ceramides (F). Data are mean ± SD. *$P < 0.001$ compared with siControl.

ORMDL1, -2, or -3 induced an increase in N-acyl chain-only [^{13}C]labeled C16:0 and C18:0 dihydroceramide species (Fig. 4C), likely due to elongation of the labeled palmitate and subsequent reacylation of unlabeled dihydrosphingosine. Consistent with results in Figs. 1, 2, only siORMDL3 increased unlabeled dihydroceramides (Fig. 4D) as well as dramatically increasing base-only and dual-labeled ceramide species (Fig. 4E, F).

Inflammatory cytokines important for the APR decrease ORMDL protein and increase dihyroceramides and ceramides

Earlier studies demonstrated that ceramide is elevated during APR (10), the early innate response to infections and inflammation. In addition to activation of neutral sphingomyelinase (27, 28), liver APR induced by LPS led to increased de novo synthesis of ceramide by increasing expression and activity of SPT (11). Moreover, key inducers and mediators of APR, including IL-1 and IL-6, induced early generation of ceramide in primary hepatocytes (6, 7). Because HepG2 cells are a suitable in vitro model system for the study of human hepatocytes, we next examined the effects of IL-1 together with OSM, a potent member of the IL-6 cytokine family that profoundly regulates APP expression (29), on ceramide levels and ORMDL expression in HepG2 cells that abundantly express receptors for both IL-1 and OSM. Stimulation with IL-1 and OSM induced small but significant increases in the level of 24:1 dihydroceramide (**Fig. 5A**) and greater increases in several species of ceramides (Fig. 5B). Moreover, dihydrosphingosine and sphingosine, as well as S1P, were also increased (Fig. 5C). Although, as expected, IL-1 and OSM increased transcription of the APP, SAA1 (Fig. 5D), no changes were detected in mRNA levels of ORMDL1, ORMDL2, or ORMDL3 (Fig. 5D). Interestingly, stimulation of HepG2 cells with IL-1 and OSM caused a significant decrease in ORMDL protein detected by immunoblotting (Fig. 5E), suggesting that this may be due to increased degradation. The decrease in

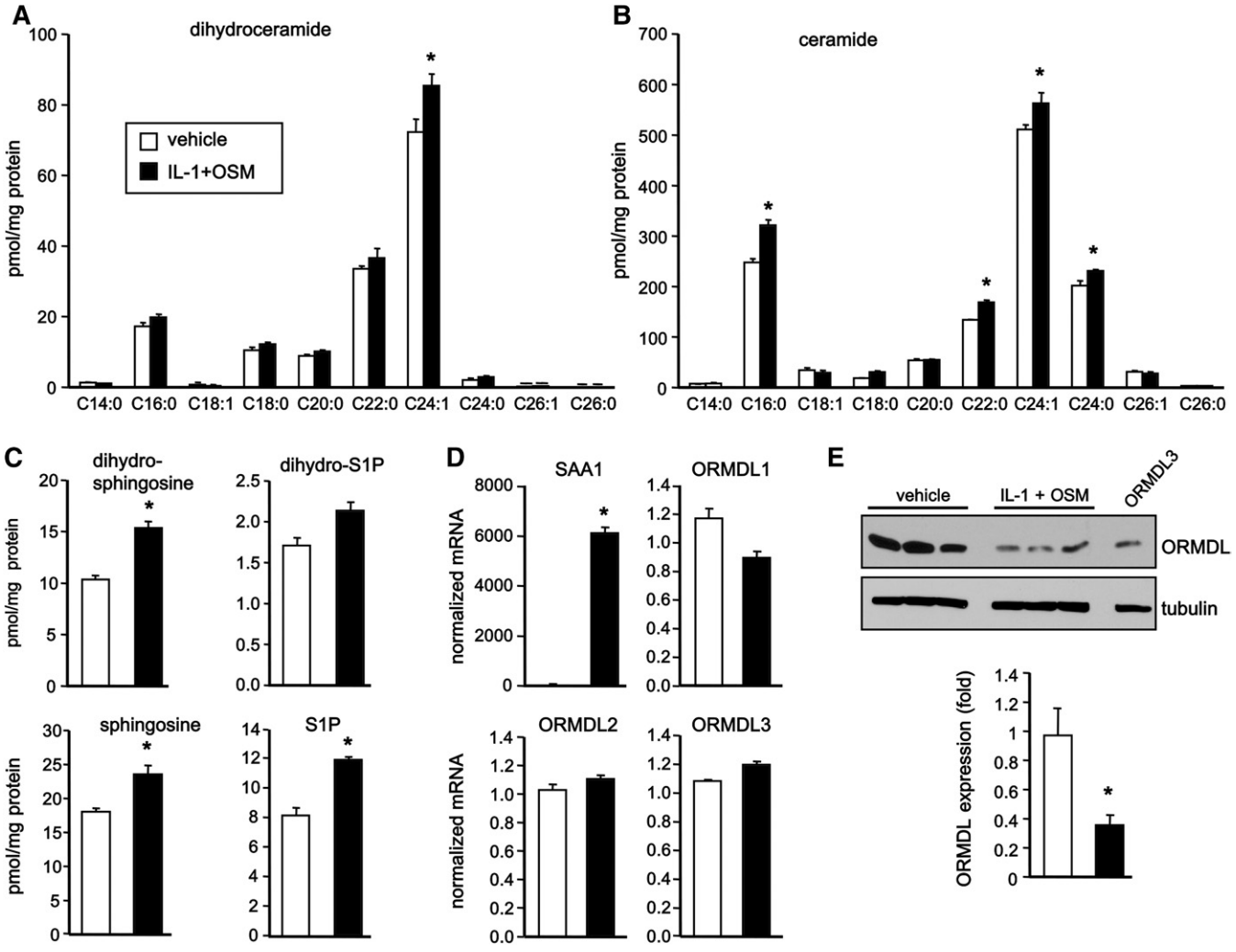

Fig. 5. Pro-inflammatory cytokines increase ceramides and dihydroceramides concurrently with decreased ORMDL protein. A–E: HepG2 cells were treated with vehicle or IL-1 plus OSM for 24 h. Lipids were extracted and ceramide species (A), dihydroceramide species (B), and dihydrosphingosine, dihydro-S1P, sphingosine, and S1P (C) were quantified by LC-ESI-MS/MS. D: mRNA levels of SAA1 and individual ORMDLs were determined by QPCR and normalized to GAPDH. E: Cell lysates were analyzed by immunoblotting with ORMDL3 antibody. Blots were probed with anti-tubulin antibody to ensure equal loading and transfer and quantified by densitometry (n = 7). Data are mean ± SD. *$P < 0.001$ compared with untreated control.

ORMDL protein expression is consistent with the increases in dihydroceramides and ceramides.

Irritant-induced inflammation decreased ORMDL protein expression and increased ceramides and dihydroceramides in the liver

To examine the effect on ORMDL expression during APR, we used a mouse model of irritant-induced acute inflammation that is IL-1-dependent (4). In this model, sc injection of turpentine causes tissue destruction at the site of injection, infiltration of inflammatory cells, and production of cytokines, including IL-1 and OSM (23). This is followed by a systemic response and production of APPs in the liver (30). Indeed, turpentine induced significant increases in transcription within 8 h of the classical markers of liver inflammation, SAA1, serum amyloid protein, and α-1-acid glycoprotein (**Fig. 6A**), all proteins secreted by the liver into the serum in response to inflammatory signals, such as IL-1 and OSM (31). Although no changes were observed in mRNA levels of any of the ORMDLs, as measured by quantitative (Q)PCR (Fig. 6A), turpentine treatment also induced a significant decrease in ORMDL protein levels within 8 h, which remained reduced after 24 h (Fig. 6B). Consistent with this decrease in ORMDLs, liver levels of dihydroceramides (**Fig. 7A**) and ceramides (Fig. 7B) were significantly increased by turpentine and generally evenly distributed across all acyl chain species. Although no major changes were observed in levels of dihydrosphingomyelins or sphingomyelins (Fig. 7A, B), significant increases, especially after 24 h, were observed in some monohexosyldihydroceramide and monohexosylceramide species (Fig. 7A, B). However, there were no significant changes in sphingoid bases or their phosphorylated forms (Fig. 7C).

A portion of the de novo generated ceramide in the liver is secreted into blood as components of VLDLs and LDLs. Because changes in hepatic SPT activity affect the rate of ceramide secretion (11), we also measured the effects of turpentine treatment on sphingolipid levels in blood. At 8 h following treatment with turpentine, there were only minor effects on levels of dihydroceramides and ceramides (**Fig. 8A, B**). However, after 24 h, there were significant increases in dihydroceramides (Fig. 8A) and more pronounced increases in ceramides, particularly C22:0, C24:1, and C24:0 species (Fig. 8B). Dihydrosphingomyelins and sphingomyelins (Fig. 8A, B) were not greatly affected by turpentine, although there were robust increases after 24 h in monohexosyldihydroceramides and monohexosylceramides (Fig. 8A, B). At this time point, there were also small increases in blood levels of phosphorylated sphingoid bases (Fig. 8C).

DISCUSSION

Here we demonstrated that decreasing expression of ORMDL3 in liver cells, but not ORMDL1 or -2, induced a dramatic increase in dihydrosphingosine and dihydrosphingosine-containing sphingolipids. Dihydrosphingosine is an intermediate in the de novo pathway, suggesting that ORMDL3, similar to its yeast homologs, is a homeostatic negative regulator of SPT, the first committed step in sphingolipid synthesis. This is consistent with our previous findings in lung epithelial cells (20), but in contrast to another report in HEK293 cells suggesting that all three ORMDL isoforms must be downregulated to relieve the inhibition of SPT (21). Although the explanation for this discrepancy is not clear, it may be due to distinct functions

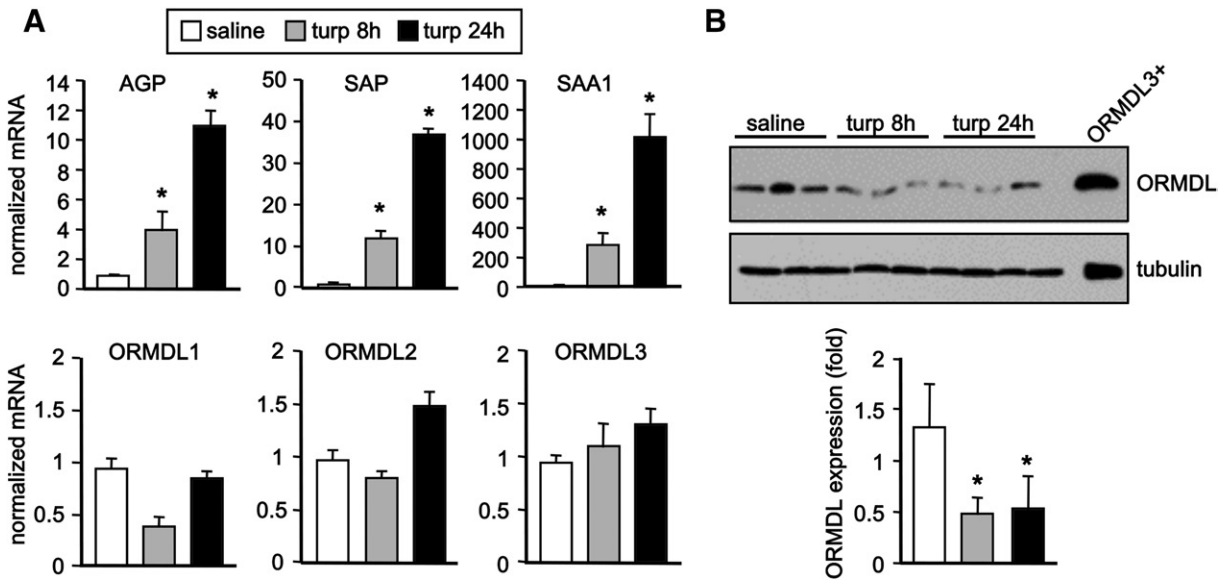

Fig. 6. Sterile inflammation in mice decreases ORMDL protein expression. Mice were injected sc with 50 μl turpentine or saline (n = 3 in each group). Livers were isolated after 8 and 24 h. A: mRNA levels of SAA1, serum amyloid protein (SAP), α-1-acid glycoprotein (AGP), and ORMDL1–3 were determined by QPCR and normalized to GAPDH. B: Liver proteins were separated by SDS-PAGE and immunoblotted with anti-ORMDL3 antibody. Blots were probed with anti-tubulin to ensure equal transfer and loading and quantified by densitometry (n = 3). Data are mean ± SD. *$P < 0.01$ compared with saline-treated control.

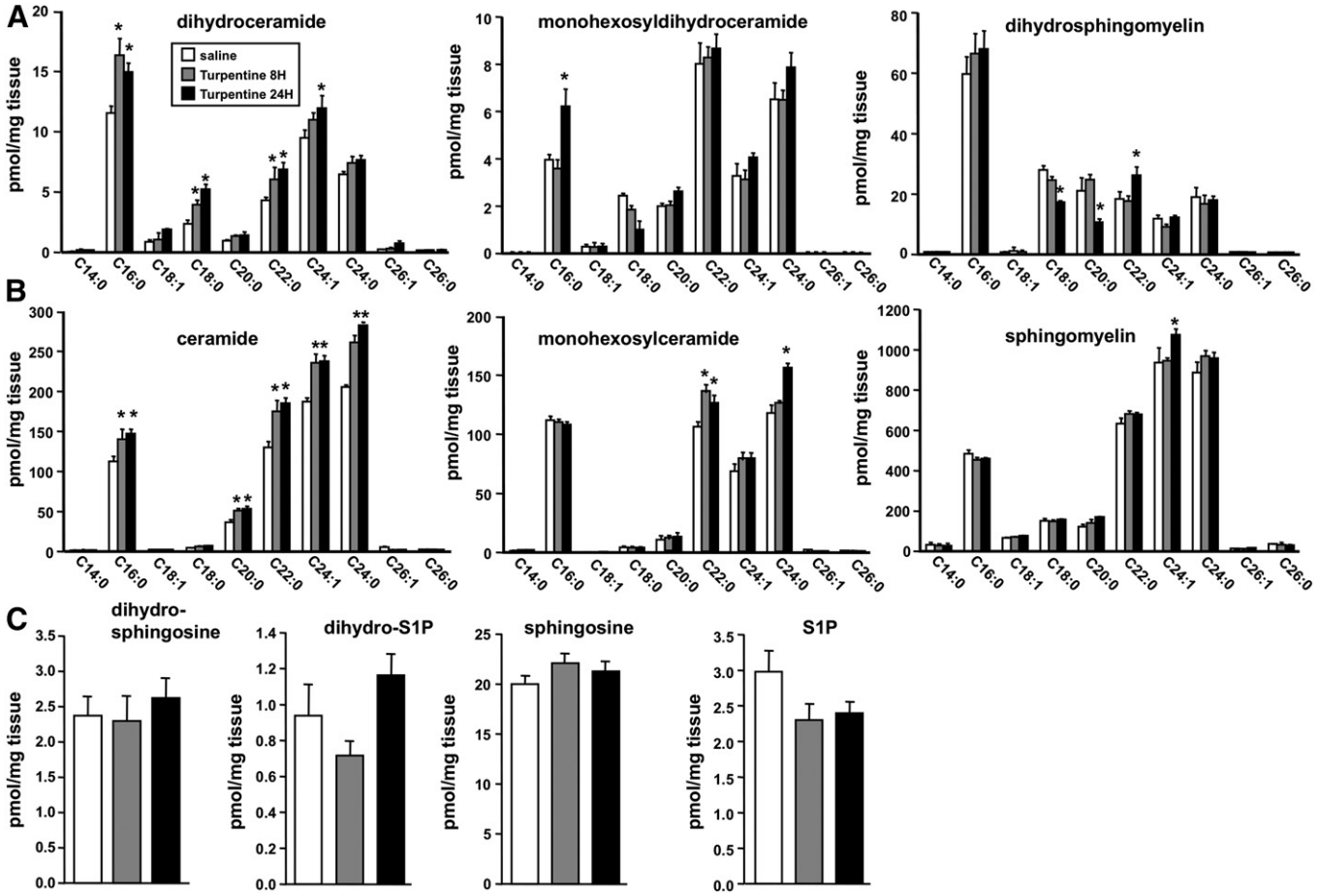

Fig. 7. Sterile inflammation in mice increases dihydroceramide and ceramide in liver. Mice were injected with turpentine or saline (n = 3), as described in Fig. 6. Lipids were extracted from livers and levels of dihydroceramides, monohexosyldihydroceramides, and dihydrosphingomyelins (A), ceramides, monohexosylceramides, and sphingomyelins (B), and dihydrosphingosine, dihydro-S1P, sphingosine, and S1P (C) were measured by LC-ESI-MS/MS. Data are mean ± SD. $*P < 0.001$ compared with saline control.

of ORMDLs in different cell types. It is also possible that ORMDL3 expression is relatively higher than the other ORMDLs in certain cell types, such as liver cells. A more likely explanation is that our highly sensitive and precise LC-ESI-MS/MS methods more accurately measure small changes in sphingolipid levels. However, it is also possible that there are small changes in different subcellular pools of sphingolipids. Indeed, whereas total ceramides were only increased with siORMDL3, pulse-labeling experiments with [^{13}C]palmitate demonstrated that downregulation of ORMDL1, -2, or -3 induced comparable increases in palmitic acid-labeled dihydroceramide, suggesting that although ORMDL1 or ORMDL2 may not regulate bulk sphingolipid levels, they could play a role in the regulation of specific pools of dihydroceramides and/or recycling.

It must be noted that we did observe that knockdown of all three ORMDL proteins simultaneously had a stronger effect on levels of dihydrosphingosine and dihydrosphingosine-containing lipids than knockdown of ORMDL3 alone. This also supports the notion that while ORMDL3 is a strong and potentially physiologically relevant control node for regulation of sphingolipid biosynthesis, the three ORMDL proteins may have overlapping functions. As expected from the increased levels of sphingolipids, we observed that decreased ORMDL3 expression increased levels of free sphingoid bases and sphingoid base phosphates, and also caused increases in cellular levels of ceramides. Levels of complex sphingolipids were also increased, though to a lesser extent, likely due both to the large pools of these sphingolipids within the cell and the relatively short times of knockdown.

Intriguingly, although ORMDL1 had no effect on dihydrosphingosine or dihydrosphingosine-containing sphingolipids, we found that its downregulation modestly increased levels of sphingosine, S1P, and ceramide. Thus, ORMDL1 may act downstream of SPT in mammalian cells. Support for this idea comes from the demonstration that in yeast, the ORMDL homolog, ORM1, forms a complex not only with SPT but also with the yeast ceramide synthase homolog, Lac1 (16), suggesting an additional role for the ORMs in regulating sphingolipid homeostasis. In agreement, it was shown in yeast that ORMs have two separate functions in sphingolipid metabolism: inhibition of SPT and activation of complex sphingolipid synthesis (17).

Nevertheless, the ratio of total sphingosine- to dihydrosphingosine-containing sphingolipids was decreased in triple ORMDL knockdown by 4-fold for ceramide/dihydroceramide, but only by 2-fold for complex sphingolipid

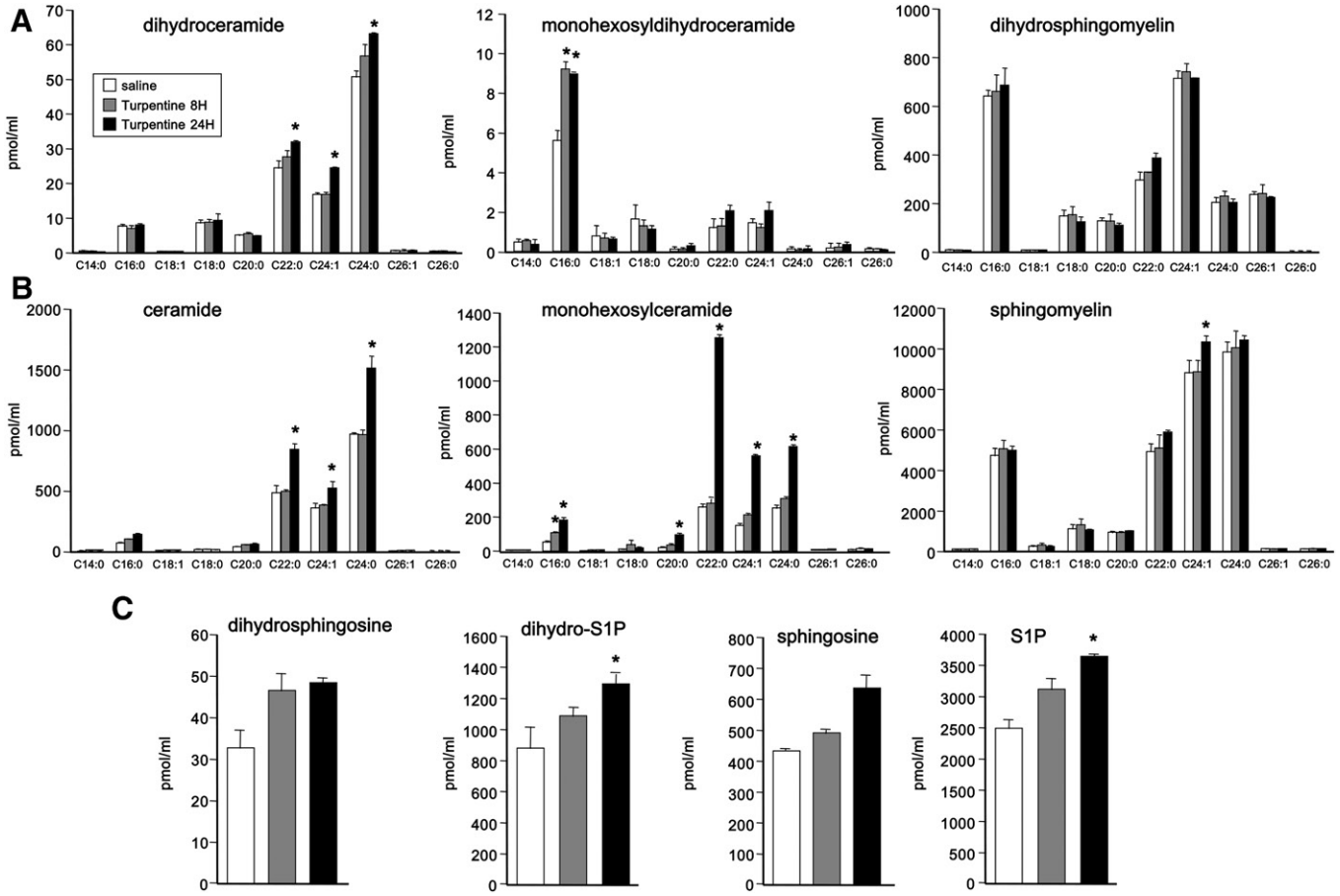

Fig. 8. Effect of turpentine-induced sterile inflammation on serum sphingolipid levels. Mice were injected sc with 50 μl turpentine or saline (n = 3). Eight and 24 h later, lipids were extracted from blood and levels of dihydroceramides, monohexosyldihydroceramides, and dihydrosphingomyelins (A), ceramides, monohexosylceramides, and sphingomyelins (B), and dihydrosphingosine, dihydro-S1P, sphingosine, and S1P (C) were measured by LC-ESI-MS/MS. Data are mean ± SD. *$P < 0.001$ compared with saline control.

species, again indicative of an increase in de novo SPT-initiated sphingolipid synthesis. Likewise, increased levels of dihydrosphingosine-containing sphingolipids were observed in most acyl chain species, suggesting that the changes induced by ORMDL knockdown occur before the acyl chain is added, that is, at the stage of formation of the sphingoid base itself.

Numerous genome-wide association studies have linked ORMDL3 SNPs to increased risk of asthma development (32, 33), while others have linked them to inflammatory disorders, including colitis, diabetes, and atherosclerosis (34, 35). Therefore, we examined whether ORMDL expression is modulated physiologically during inflammatory responses. This has clinical significance as elevated levels of ceramide have been associated with induction and propagation of inflammatory responses (2). In this regard, we found that inflammatory cytokines reduced levels of ORMDL protein in liver cells concomitant with increased levels of ceramide and other sphingolipids, including dihydroceramide, sphingoid bases, and sphingoid base phosphates. Combination of IL-1 and OSM significantly reduced ORMDL protein levels, although each alone did not. The synergistic effect of IL-1 and OSM on ORMDL expression is likely physiologically significant because both IL-1 and OSM also synergistically control expression of type 1 APPs (29). The changes in ORMDL protein levels, but not in mRNA levels, indicate posttranscriptional regulation of ORMDL protein levels. These results are consistent with those in yeast, in which the levels of the ORMDL homolog, ORM2, are decreased in response to endoplasmic reticulum stress (16). Moreover, it was recently shown that ORMDL proteins are degraded by cholesterol loading-induced autophagy (36). In addition, during irritant-induced APR in mice mediated by IL-1-dependent sterile injury, we noted that ORMDL proteins were also decreased in the liver, once again without affecting mRNA levels, and dihydroceramides and ceramides were increased in liver and accumulated in the circulation. In addition, the changes in dihydroceramide and ceramide species observed in both liver and blood during APR were generally proportional to their abundance, with larger changes occurring in more abundant N-acyl chain species. Although sterile inflammation in vivo is much more complicated than effects of IL-1 and OSM on cultured cells, taken together, these results support the notion that ORMDLs may modulate SPT-dependent de novo sphingolipid biosynthesis in IL-1-mediated sterile inflammation. Liver diseases caused by sterile inflammation contribute to many liver pathologies

and specific therapies are still needed. Understanding the involvement of ORMDLs and sphingolipid metabolites in IL-1 signaling pathways may lead to the discovery of new therapeutic targets.

REFERENCES

1. Hannun, Y. A., and L. M. Obeid. 2008. Principles of bioactive lipid signalling: lessons from sphingolipids. *Nat. Rev. Mol. Cell Biol.* **9:** 139–150.
2. Maceyka, M., and S. Spiegel. 2014. Sphingolipid metabolites in inflammatory disease. *Nature.* **510:** 58–67.
3. Kubes, P., and W. Z. Mehal. 2012. Sterile inflammation in the liver. *Gastroenterology.* **143:** 1158–1172.
4. Leon, L. R., C. A. Conn, M. Glaccum, and M. J. Kluger. 1996. IL-1 type I receptor mediates acute phase response to turpentine, but not lipopolysaccharide, in mice. *Am. J. Physiol.* **271:** R1668–R1675.
5. Baumann, H., and J. Gauldie. 1994. The acute phase response. *Immunol. Today.* **15:** 74–80.
6. Chen, J., M. Nikolova-Karakashian, A. H. Merrill, Jr., and E. T. Morgan. 1995. Regulation of cytochrome P450 2C11 (CYP2C11) gene expression by interleukin-1, sphingomyelin hydrolysis, and ceramides in rat hepatocytes. *J. Biol. Chem.* **270:** 25233–25238.
7. Nikolova-Karakashian, M., E. T. Morgan, C. Alexander, D. C. Liotta, and A. H. Merrill, Jr. 1997. Bimodal regulation of ceramidase by interleukin-1beta. Implications for the regulation of cytochrome p450 2C11. *J. Biol. Chem.* **272:** 18718–18724.
8. Giltiay, N. V., A. A. Karakashian, A. P. Alimov, S. Ligthle, and M. N. Nikolova-Karakashian. 2005. Ceramide- and ERK-dependent pathway for the activation of CCAAT/enhancer binding protein by interleukin-1beta in hepatocytes. *J. Lipid Res.* **46:** 2497–2505.
9. Dobierzewska, A., L. Shi, A. A. Karakashian, and M. N. Nikolova-Karakashian. 2012. Interleukin 1beta regulation of FoxO1 protein content and localization: evidence for a novel ceramide-dependent mechanism. *J. Biol. Chem.* **287:** 44749–44760.
10. Lightle, S., R. Tosheva, A. Lee, J. Queen-Baker, B. Boyanovsky, S. Shedlofsky, and M. Nikolova-Karakashian. 2003. Elevation of ceramide in serum lipoproteins during acute phase response in humans and mice: role of serine-palmitoyl transferase. *Arch. Biochem. Biophys.* **419:** 120–128.
11. Memon, R. A., W. M. Holleran, A. H. Moser, T. Seki, Y. Uchida, J. Fuller, J. K. Shigenaga, C. Grunfeld, and K. R. Feingold. 1998. Endotoxin and cytokines increase hepatic sphingolipid biosynthesis and produce lipoproteins enriched in ceramides and sphingomyelin. *Arterioscler. Thromb. Vasc. Biol.* **18:** 1257–1265.
12. Lowther, J., J. H. Naismith, T. M. Dunn, and D. J. Campopiano. 2012. Structural, mechanistic and regulatory studies of serine palmitoyltransferase. *Biochem. Soc. Trans.* **40:** 547–554.
13. Breslow, D. K., S. R. Collins, B. Bodenmiller, R. Aebersold, K. Simons, A. Shevchenko, C. S. Ejsing, and J. S. Weissman. 2010. Orm family proteins mediate sphingolipid homeostasis. *Nature.* **463:** 1048–1053.
14. Roelants, F. M., D. K. Breslow, A. Muir, J. S. Weissman, and J. Thorner. 2011. Protein kinase Ypk1 phosphorylates regulatory proteins Orm1 and Orm2 to control sphingolipid homeostasis in Saccharomyces cerevisiae. *Proc. Natl. Acad. Sci. USA.* **108:** 19222–19227.
15. Han, S., M. A. Lone, R. Schneiter, and A. Chang. 2010. Orm1 and Orm2 are conserved endoplasmic reticulum membrane proteins regulating lipid homeostasis and protein quality control. *Proc. Natl. Acad. Sci. USA.* **107:** 5851–5856.
16. Liu, M., C. Huang, S. R. Polu, R. Schneiter, and A. Chang. 2012. Regulation of sphingolipid synthesis through Orm1 and Orm2 in yeast. *J. Cell Sci.* **125:** 2428–2435.
17. Shimobayashi, M., W. Oppliger, S. Moes, P. Jeno, and M. N. Hall. 2013. TORC1-regulated protein kinase Npr1 phosphorylates Orm to stimulate complex sphingolipid synthesis. *Mol. Biol. Cell.* **24:** 870–881.
18. Gururaj, C., R. Federman, and A. Chang. 2013. Orm proteins integrate multiple signals to maintain sphingolipid homeostasis. *J. Biol. Chem.* **288:** 20453–20463. [Erratum. 2015. *J. Biol. Chem.* **290:** 1455.]
19. Siow, D., M. Sunkara, T. M. Dunn, A. J. Morris, and B. Wattenberg. 2015. ORMDL/serine palmitoyltransferase stoichiometry determines effects of ORMDL3 expression on sphingolipid biosynthesis. *J. Lipid Res.* **56:** 898–908.
20. Oyeniran, C., J. L. Sturgill, N. C. Hait, W. C. Huang, D. Avni, M. Maceyka, J. Newton, J. C. Allegood, A. Montpetit, D. H. Conrad, et al. 2015. Aberrant ORM (yeast)-like protein isoform 3 (ORMDL3) expression dysregulates ceramide homeostasis in cells and ceramide exacerbates allergic asthma in mice. *J. Allergy Clin. Immunol.* **136:** 1035.e6–1046.e6.
21. Kiefer, K., A. Carreras-Sureda, R. Garcia-Lopez, F. Rubio-Moscardo, J. Casas, G. Fabrias, and R. Vicente. 2015. Coordinated regulation of the orosomucoid-like gene family expression controls de novo ceramide synthesis in mammalian cells. *J. Biol. Chem.* **290:** 2822–2830.
22. Siow, D. L., and B. W. Wattenberg. 2012. Mammalian ORMDL proteins mediate the feedback response in ceramide biosynthesis. *J. Biol. Chem.* **287:** 40198–40204.
23. Harikumar, K. B., J. W. Yester, M. J. Surace, C. Oyeniran, M. M. Price, W-C. Huang, N. C. Hait, J. C. Allegood, A. Yamada, X. Kong, et al. 2014. K63-linked polyubiquitination of transcription factor IRF1 is essential for IL-1-induced production of chemokines CXCL10 and CCL5. *Nat. Immunol.* **15:** 231–238.
24. Sims, K., C. A. Haynes, S. Kelly, J. C. Allegood, E. Wang, A. Momin, M. Leipelt, D. Reichart, C. K. Glass, M. C. Sullards, et al. 2010. Kdo2-lipid A, a TLR4-specific agonist, induces de novo sphingolipid biosynthesis in RAW264.7 macrophages, which is essential for induction of autophagy. *J. Biol. Chem.* **285:** 38568–38579.
25. Haynes, C. A., J. C. Allegood, E. W. Wang, S. L. Kelly, M. C. Sullards, and A. H. Merrill, Jr. 2011. Factors to consider in using [U-C]palmitate for analysis of sphingolipid biosynthesis by tandem mass spectrometry. *J. Lipid Res.* **52:** 1583–1594.
26. Gupta, S. D., K. Gable, A. Alexaki, P. Chandris, R. L. Proia, T. M. Dunn, and J. M. Harmon. 2015. Expression of the ORMDLS, modulators of serine palmitoyltransferase, is regulated by sphingolipids in mammalian cells. *J. Biol. Chem.* **290:** 90–98.
27. Karakashian, A. A., N. V. Giltiay, G. M. Smith, and M. N. Nikolova-Karakashian. 2004. Expression of neutral sphingomyelinase-2 (NSMase-2) in primary rat hepatocytes modulates IL-beta-induced JNK activation. *FASEB J.* **18:** 968–970.
28. Nikolova-Karakashian, M., A. Karakashian, and K. Rutkute. 2008. Role of neutral sphingomyelinases in aging and inflammation. *Subcell. Biochem.* **49:** 469–486.
29. Richards, C. D., T. J. Brown, M. Shoyab, H. Baumann, and J. Gauldie. 1992. Recombinant oncostatin M stimulates the production of acute phase proteins in HepG2 cells and rat primary hepatocytes in vitro. *J. Immunol.* **148:** 1731–1736.
30. Glibetic, M. D., and H. Baumann. 1986. Influence of chronic inflammation on the level of mRNA for acute-phase reactants in the mouse liver. *J. Immunol.* **137:** 1616–1622.
31. Bode, J. G., U. Albrecht, D. Haussinger, P. C. Heinrich, and F. Schaper. 2012. Hepatic acute phase proteins–regulation by IL-6- and IL-1-type cytokines involving STAT3 and its crosstalk with NF-kappaB-dependent signaling. *Eur. J. Cell Biol.* **91:** 496–505.
32. Moffatt, M. F., M. Kabesch, L. Liang, A. L. Dixon, D. Strachan, S. Heath, M. Depner, A. von Berg, A. Bufe, E. Rietschel, et al. 2007. Genetic variants regulating ORMDL3 expression contribute to the risk of childhood asthma. *Nature.* **448:** 470–473.
33. Schedel, M., S. Michel, V. D. Gaertner, A. A. Toncheva, M. Depner, A. Binia, M. Schieck, M. T. Rieger, N. Klopp, A. von Berg, et al. 2015. Polymorphisms related to ORMDL3 are associated with asthma susceptibility, alterations in transcriptional regulation of ORMDL3, and changes in T2 cytokine levels. *J. Allergy Clin. Immunol.* **136:** 893.e14–903.e14.
34. McGovern, D. P., A. Gardet, L. Torkvist, P. Goyette, J. Essers, K. D. Taylor, B. M. Neale, R. T. Ong, C. Lagace, C. Li, et al. 2010. Genome-wide association identifies multiple ulcerative colitis susceptibility loci. *Nat. Genet.* **42:** 332–337.
35. Ma, X., R. Qiu, J. Dang, J. Li, Q. Hu, S. Shan, Q. Xin, W. Pan, X. Bian, Q. Yuan, et al. 2015. ORMDL3 contributes to the risk of atherosclerosis in Chinese Han population and mediates oxidized low-density lipoprotein-induced autophagy in endothelial cells. *Sci. Rep.* **5:** 17194.
36. Wang, S., P. Robinet, J. D. Smith, and K. Gulshan. 2015. ORMDL orosomucoid-like proteins are degraded by free-cholesterol-loading-induced autophagy. *Proc. Natl. Acad. Sci. USA.* **112:** 3728–3733.